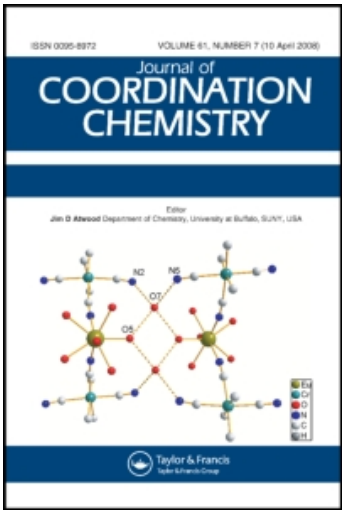

Journal of Coordination Chemistry
Publication details, including instructions for authors and subscription information:
http://www.informaworld.com/smpp/title~content=t713455674

The crystal structure of braithwaiteite

Frank C. Hawthorne[a]; Mark A. Cooper[a]; Werner H. Paar[b]
[a] Department of Geological Sciences, University of Manitoba, Winnipeg, Manitoba R3T 2N2, Canada [b] Department of Material Science (Applied Mineralogy), University of Salzburg, Hellbrunnerstr. 34, A-5020 Salzburg, Austria

To cite this Article Hawthorne, Frank C. , Cooper, Mark A. and Paar, Werner H.(2008) 'The crystal structure of braithwaiteite', Journal of Coordination Chemistry, 61: 1, 15 — 29
To link to this Article: DOI: 10.1080/00958970701700961
URL: http://dx.doi.org/10.1080/00958970701700961

Journal of Coordination Chemistry
Vol. 61, No. 1, 10 January 2008, 15–29

Taylor & Francis
Taylor & Francis Group

The crystal structure of braithwaiteite

FRANK C. HAWTHORNE*†, MARK A. COOPER†
and WERNER H. PAAR‡

†Department of Geological Sciences, University of Manitoba, Winnipeg, Manitoba R3T 2N2, Canada
‡Department of Material Science (Applied Mineralogy), University of Salzburg, Hellbrunnerstr. 34, A-5020 Salzburg, Austria

(*Received 7 June 2007; in final form 6 August 2007*)

The crystal structure of braithwaiteite, $NaCu^{2+}{}_5(Sb^{5+}Ti^{4+})O_2(AsO_4)_4(AsO_3OH)_2(H_2O)_8$, triclinic, $Z=1$, $P\bar{1}$, $a=7.0308(4)$, $b=9.8823(5)$, $c=10.6754(6)$Å, $\alpha=106.973(1)$, $\beta=104.274(1)$, $\gamma=93.839(1)^\circ$, $V=679.76(11)$ Å^3, was solved by direct methods and refined to an R_1 index of 0.025 for 3584 observed reflections. A prominent motif in the braithwaiteite structure is a chain of corner-sharing (Sb,TiO_6) octahedra that is decorated with (AsO_4) tetrahedra to form a $[(SbTi)(AsO_4)_4O_2]$ chain that extends along the ***a***-direction and defines the cell dimension in this direction at ~7 Å. These chains are cross-linked in the ***b***-direction by chains of edge-sharing (CuO_6) octahedra that are decorated by arsenate tetrahedra to form a $[Cu_2(AsO_4OH)_2O_4]$ chain; these two chains link to form a sheet parallel to (001). These sheets stack along the ***c***-direction and are linked by (CuO_6) and (NaO_6) octahedra, together with an extensive network of hydrogen bonds. The $[M(TO_4)_2\Phi_4]$ chain (M = octahedrally coordinated metal, T = tetrahedrally coordinated metal, Φ = unspecified simple anion; $\equiv[(SbTi)(AsO_4)_4O_2]$ chain) is a common motif in secondary oxysalt minerals, occurring in sulfates, phosphates, arsenates, vanadates and silicates.

Keywords: Braitwaiteite; Crystal structure; Oxysalt mineral

1. Introduction

Braithwaiteite is a new mineral which occurs in trace amounts on an old specimen of the *Veta Negra* (Black Vein), Laurani, Bolivia, a high sulfidation (''HS'') epithermal deposit at the western border of the Bolivian tin province near Sica Sica. This specimen is also the holotype specimen for lammerite, $Cu^{2+}{}_3(AsO_4)_2$ [1, 2] and is described in detail [1]. Braithwaiteite is a secondary mineral formed by oxidation of primary enargite by Ti- and Na-bearing fluids in an arid environment. Associated minerals are lammerite, lavendulan, enargite (containing 5–7 wt% Sb), pyrite, covellite, anatase, albite-oligoclase, chlorite and quartz. The formula, $NaCu^{2+}{}_5(Sb^{5+}Ti^{4+})O_2(AsO_4)_4(AsO_3OH)_2(H_2O)_8$, established by electron-microprobe analysis and crystal-structure solution and refinement, is typical of the secondary oxysalt minerals that have been one of Peter Williams' major scientific interests [e.g. 3, 4, 5, 6]. Here, we present

*Corresponding author. Email: frank_hawthorne@umanitoba.ca

Journal of Coordination Chemistry
ISSN 0095-8972 print/ISSN 1029-0389 online © 2008 Taylor & Francis
DOI: 10.1080/00958970701700961

the crystal structure of braithwaiteite and examine its structural relations with other secondary oxysalt minerals.

2. Experimental

2.1. *Material*

There is a paucity of material for this work. Only two crystal aggregates, each less than 1 mm in size, were found, and one crystal ($0.015 \times 0.100 \times 0.150$ mm) was used for the entire investigation.

2.2. *Apparatus*

Single-crystal X-ray diffraction data were collected with Mo$K\alpha$ X-radiation on a Bruker 4-circle diffractometer equipped with an APEX 4K CCD detector. In excess of a sphere of data was collected to 60° 2θ using a frame time of 60s and frame width of 0.3°. The data were corrected for Lorentz, polarization, background and absorption (SADABS) effects, resulting in 3584 observed ($|F_o| > 4|F|$) reflections. The unit cell is based on 7503 reflections ($> 10\sigma I$).

2.3. *Structure solution and refinement*

The crystal structure of braithwaiteite was solved in the space group $P\bar{1}$ by direct methods using the SHELXTL 4.2 software package for Bruker Analytical X-ray Systems [7]. The final model had anisotropic-displacement parameters for all non-H atoms and variable (Sb,Ti) occupancies for the two *M* sites, and refined to an R_1 index of 0.025 for 3584 observed reflections.

3. Results and discussion

Atom positions and displacement parameters are available in supplementary data, selected interatomic distances and angles are given in table 1, and bond valences, calculated with the parameters listed in [8], are given in table 2.

3.1. *Local structure*

There are three As sites occupied by As (see supplementary data). The tetrahedral coordination and <As–O> distances (see table 1) are compatible with As^{5+} at each site, and this is confirmed by the bond-valence sums (see table 2) which are close to their ideal value of 5 vu (valence units). There are four Cu sites, each of which is occupied by Cu with <Cu–O> distances in the range 1.90–3.17 Å. The four short and two long distances, [4 + 2]-coordination, of each Cu octahedron is typical of Jahn-Teller distortion around Cu^{2+} in octahedral coordination [9]. Moreover, the differences

Table 1. Selected interatomic distances (Å) and angles in braithwaiteite.

Na–O(9)*f*,*h*	x2	2.373(2)	As(1)–O(1)		1.698(3)
Na–OW(3),*j*	x2	2.349(5)	As(1)–O(2)		1.689(2)
Na–OW(4),*j*	x2	2.412(5)	As(1)–O(3)		1.677(3)
<Na–O>		2.378	As(1)–O(4)		1.691(3)
			<As(1)–O>		1.689
Cu(1)–O(3),*c*	x2	2.519(3)			
Cu(1)–O(8),*c*	x2	1.957(3)	As(2)–*O*(5)		1.715(3)
Cu(1)–O(11),*c*	x2	1.990(3)	As(2)–*O*(6)		1.704(3)
<Cu(1)–O>		2.155	As(2)–*O*(7)		1.672(3)
			As(2)–*O*(8)*g*		1.669(3)
Cu(2)–O(7)*e*,*f*	x2	1.902(4)	<As(2)–O>		1.690
Cu(2)–OW(1),*i*	x2	2.024(3)			
Cu(2)–OW(2),*i*	x2	2.739(4)	As(3)–O(9)		1.678(3)
<Cu(2)–O>		2.222	As(3)–O(10)		1.690(3)
			As(3)–O(11)		1.670(2)
Cu(3)–O(3),*b*	x2	2.002(3)	As(3)–O(12)		1.709(3)
Cu(3)–O(6),*b*	x2	1.931(3)	<As(3)–O>		1.687
Cu(3)–O(11),*b*	x2	2.484(3)			
<Cu(3)–O>		2.139	M(1)–O(4),*d*	x2	2.000(3)
			M(1)–O(10)*b*,*h*	x2	1.968(3)
Cu(4)–O(2)		1.905(3)	M(1)–O(13),*d*	x2	1.889(3)
Cu(4)–O(3)		3.151(2)	<*M*(1)–O>		1.952
Cu(4)–O(6)		2.051(3)			
Cu(4)–O(7)		3.191(3)	M(2)–O(1),*a*	x2	1.999(2)
Cu(4)–O(8)		2.764(3)	M(2)–O(12)*c*,*h*	x2	2.022(3)
Cu(4)–O(9)		1.911(3)	M(2)–O(13)*d*,*e*	x2	1.863(3)
Cu(4)–O(11)		3.174(3)	<*M*(2)–O>		1.961
Cu(4)–OW(2)		1.997(4)			
<Cu(4)–0>		2.518			
O(5)–H(9)		0.98(7)	H(8)···O(12)*g*		1.81(8)
O(5)–O(12)*g*		2.737(5)	O(5)–H(9)–O(12)*g*		159(5)
OW(1)–H(1)		0.98(6)	H(1)···O(1)		1.94(6)
OW(1)–H(2)		0.98(4)	H(2)···O(4)*e*		2.00(4)
OW(1)–O(1)		2.878(5)	OW(1)–H(1)–O(1)		162(3)
OW(1)–O(4)*e*		2.944(4)	OW(1)–H(2)–O(4)*e*		163(7)
H(1)–H(2)		1.61(7)	O(1)–OW(1)–O(4)*e*		94.5(1)
H(1)–OW(1)–H(2)		112(5)			
OW(2)–H(3)		0.98(4)	H(3)···OW(4)*f*		1.72(4)
OW(2)–H(4)		0.98(5)	H(4)···O(2)*f*		1.73(6)
OW(2)–OW(4)*f*		2.699(5)	OW(2)–H(3)–OW(4)*f*		177(7)
OW(2)–O(2)*f*		2.676(4)	OW(2)–H(4)–O(2)*f*		163(6)
H(3)–H(4)		1.52(9)	OW(4)*f*–OW(2)–O(2)*f*		105.1(1)
H(3)–OW(2)–H(4)		102(5)			
OW(3)–H(5)		0.98(6)	H(5)···O(7)*f*		1.84(6)
OW(3)–H(6)		0.98(3)	H(6)···O(1)		2.36(5)
			H(6)···O(12)*h*		2.15(4)
OW(3)–O(7)*f*		2.796(6)	OW(3)–H(5)–O(7)*f*		165(6)
OW(3)–O(1)		3.137(6)	OW(3)–H(6)–O(1)		137(6)
OW(3)–O(12)*h*		2.970(4)	OW(3)–H(6)–O(12)*h*		141(6)
H(5)–H(6)		1.60(7)	O(7)*f*–OW(3)–O(1)		95.9(2)
H(5)–OW(3)–H(6)		110(5)	O(7)*f*–OW(3)–O(12)*h*		136.7(2)
OW(4)–H(7)		0.98(3)	H(7)···O(13)		2.77(4)
OW(4)–H(8)		0.98(6)	H(7)···O(10)*h*		2.01(4)
			H(8)···O(5)*h*		2.40(6)
OW(4)–O(13)		3.534(6)	H(8)···O(5)*k*		2.78(5)
OW(4)–O(10)*h*		2.939(4)	H(8)···OW(3)*j*		2.78(8)
OW(4)–O(5)*h*		2.896(5)	H(8)···OW(3)*g*		2.96(5)
OW(4)–O(5)*k*		3.473(5)			
OW(4)–OW(3)*j*		3.257(7)	OW(4)–H(7)–O(13)		136(5)
OW(4)–OW(3)*g*		3.584(7)	OW(4)–H(7)–O(10)*h*		159(6)

(*Continued*)

Table 1. Continued.

		OW(4)–H(8)–O(5)*h*	111(4)
H(7)–H(8)	1.60(7)	OW(4)–H(8)–O(5)*k*	129(5)
H(7)–OW(4)–H(8)	110(5)	OW(4)–H(8)–OW(3)*j*	111(4)
		OW(4)–H(8)–OW(3)*g*	123(6)
		O(13)–OW(4)–O(5)*h*	65.1(1)
		O(13)–OW(4)–O(5)*k*	127.7(2)
		O(13)–OW(4)–OW(3)*j*	129.5(1)
		O(13)–OW(4)–OW(3)*g*	71.0(1)
		O(10)*h*–OW(4)–O(5)*h*	65.6(1)
		O(10)*h*–OW(4)–O(5)*k*	154.2(2)
		O(10)*h*–OW(4)–OW(3)*j*	101.2(1)
		O(10)*h*–OW(4)–OW(3)*g*	63.1(1)

a: $\bar{x}$, $\bar{y}$, $\bar{z}$; *b*: $\bar{x}+1$, $\bar{y}+1$, $\bar{z}$; *c*: $\bar{x}$, $\bar{y}+1$, $\bar{z}$; *d*: $\bar{x}+1$, $\bar{y}$, $\bar{z}$; *e*: $x-1$, y, z; *f*: $\bar{x}+1$, $\bar{y}+1$, $\bar{z}+1$; *g*: $x+1$, y, z; *h*: x, $y-1$, z; *i*: $\bar{x}$; $\bar{y}+1$, $\bar{z}+1$; *j*: $\bar{x}+1$, $\bar{y}$, $\bar{z}+1$; *k*: $\bar{x}+2$, $\bar{y}+1$, $\bar{z}+1$.

in <Cu-O> observed here are in accord with the idea that the variation in mean bond lengths for certain cations in octahedral coordination [9, 10] correlates with variation of the individual bond lengths from their mean value (as measured by the root-mean-square difference from the average value). The Cu(4) site is a general position with four short bonds [$O_3(H_2O)$] from 1.91–2.05 Å and four long bonds [O_4] from 2.76–3.19 Å.

The chemical formula derived from electron-microprobe analysis of braithwaiteite (with (OH) and (H_2O) taken from the crystal-structure determination), $Na_{0.87}Cu_{5.17}(Sb_{1.15}Ti_{0.90})O_2(As_{0.98}O_4)_2(AsO_3(OH))_2(H_2O)_8$, indicates that the $M(1)$ and $M(2)$ sites are fully occupied by Ti and Sb in approximately equal amounts, and the aggregate scattering from the two sites is in accord with this. Moreover, site-occupancy refinement gave the following values: $M(1) = 0.57\,Sb + 0.43\,Ti$, $M(2) = 0.39\,Sb + 0.61\,Ti$, in reasonable accord with the measured chemical composition. The mean bond lengths at $M(1)$ and $M(2)$ are in accord with tetravalent Ti (as is the color of the mineral: sky blue) and pentavalent Sb (trivalent Sb invariably is lone-pair stereoactive). Moreover, the bond-valence sums at $M(1)$ and $M(2)$ are in reasonable accord with both these assigned valences and the refined site-occupancies. There is one octahedrally coordinated Na site occupied by Na, as indicated by the chemical analysis and the incident bond-valence sum (see table 2) calculated for occupancy by Na. The formula derived from the electron-microprobe analysis is somewhat deficient in Na relative to that in the refined structure (0.87 atoms per formula unit versus 1.0 apfu). This difference is almost certainly the result of breakdown of the sample under the electron beam during electron-microprobe analysis, a common feature of highly hydrated secondary oxysalt minerals, despite the use of a very low beam intensity.

Assignment of the anion identities can only be done by examining the incident bond-valence sums (see table 2). O(5) has an incident bond-valence sum of 1.15 vu, indicating that it is an (OH) group which forms a hydrogen bond of intermediate strength. OW(1)–OW(4) have incident bond-valence sums of 0.18–0.48 vu, indicating that these are all (H_2O) groups which also form hydrogen bonds of intermediate strength. The ideal chemical formula that results from this structure is $NaCu^{2+}{}_5(Sb^{5+}Ti^{4+})O_2(AsO_4)_4(AsO_3OH)_2(H_2O)_8$ with $Z = 1$.

Table 2. Bond–valence table for braithwaiteite.

	As(1)	As(2)	As(3)	Cu(1)	Cu(2)	Cu(3)	Cu(4)	Na	*M*(1)	*M*(2)	Sum	H(1)	H(2)	H(3)	H(4)	H(5)	H(6)	H(7)	H(8)	H(9)	Σ
O(1)	1.21									$0.06^{x2}\downarrow$	1.87	0.14					$0.06^{x\frac{1}{2}}\downarrow\rightarrow$				2.04
O(2)	1.23						0.54				1.77				0.21						1.98
O(3)	1.28			$0.10^{x2}\downarrow$		$0.42^{x2}\downarrow$	0.02				1.82										1.82
O(4)	1.23								$0.69^{x2}\downarrow$		1.92		0.12								2.04
O(5)		1.15									1.15								$0.10^{x\frac{1}{2}}\downarrow\rightarrow$	0.82	2.02
O(6)		1.19				$0.51^{x2}\downarrow$	0.37				2.07										2.07
O(7)		1.29			$0.55^{x2}\downarrow$		0.02				1.86					0.17					2.03
O(8)		1.30		$0.47^{x2}\downarrow$			0.05				1.82										1.82
O(9)			1.27				0.53	$0.20^{x2}\downarrow$			2.00										2.00
O(10)			1.23						$0.75^{x2}\downarrow$		1.98							$0.12^{x\frac{1}{2}}\downarrow\rightarrow$			2.04
O(11)			1.30	$0.43^{x2}\downarrow$		$0.11^{x2}\downarrow$	0.02				1.86										1.86
O(12)			1.17							$0.62^{x2}\downarrow$	1.79						$0.10^{x\frac{1}{2}}\downarrow\rightarrow$			0.18	2.02
O(13)									$0.95^{x2}\downarrow$	$0.97^{x2}\downarrow$	1.92							$0.04^{x\frac{1}{2}}\downarrow\rightarrow$			1.94
OW(1)					$0.39^{x2}\downarrow$						0.39	0.86	0.88								2.13
OW(2)					$0.06^{x2}\downarrow$		0.42				0.48			0.78	0.79						2.05
OW(3)								$0.20^{x2}\downarrow$			0.20					0.83	0.92		$0.06^{x\frac{1}{2}}\downarrow\rightarrow$		1.98
OW(4)								$0.18^{x2}\downarrow$			0.18			0.22				0.92	0.92		2.24
Σ	4.95	4.93	4.97	2.00	2.00	2.08	1.97	1.16	4.78	4.50		1.00	1.00	1.00	1.00	1.00	1.00	1.00	1.00	1.00	

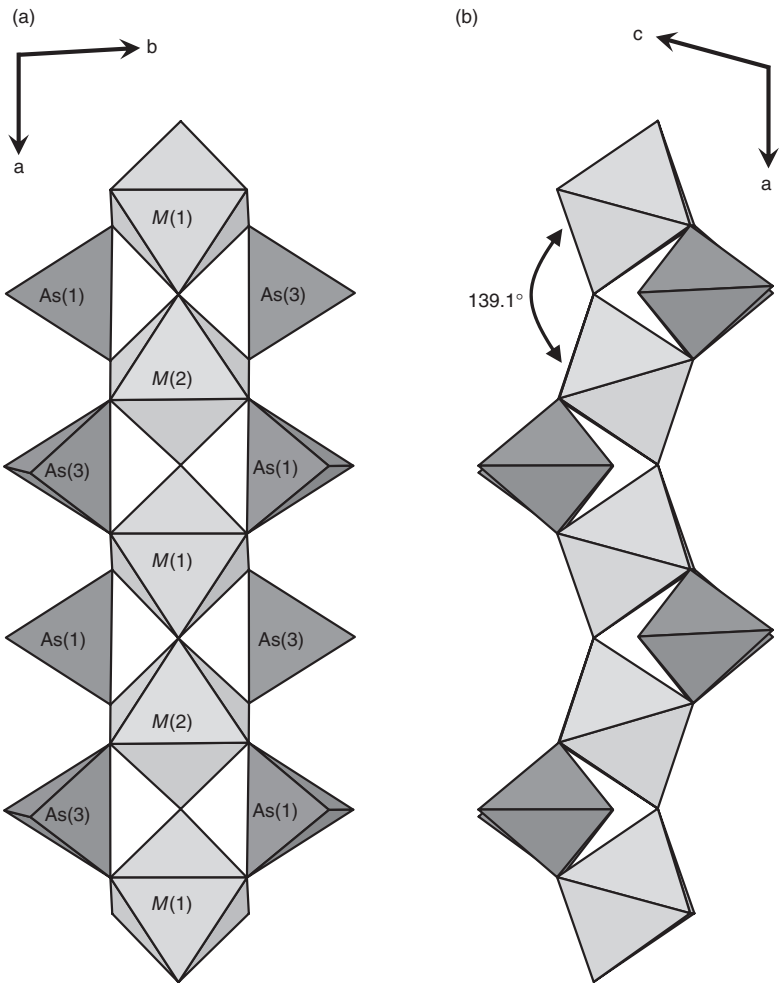

Figure 1. The $[(SbTi)(AsO_4)_4O_4]$ corner-sharing chain of $M(1)$ and $M(2)$ octahedra decorated by (AsO_4) groups in braithwaiteite (a) projected onto (001), and (b) projected onto (010).

3.2. *Extended structure*

A prominent motif in the braithwaiteite structure is the $[(SbTi)(AsO_4)_4O_2]$ chain shown in figure 1 that extends along the ***a***-direction and defines the cell dimension in this direction at ~7 Å. These chains are cross-linked in the ***b***-direction by $[Cu_2(AsO_4OH)_2O_4]$ chains of edge-sharing Cu(1) and Cu(3) octahedra that are decorated by arsenate tetrahedra, forming a sheet parallel to (001) (see figure 2). These sheets stack along the ***c***-direction and are linked by Cu(2) octahedra (see figure 3a) and Na octahedra (see figure 3b), together with an extensive network of hydrogen bonds.

3.3. *Hydrogen bonding*

The single (OH) in the braithwaiteite structure is attached to As(2), forming an acid-arsenate group $AsO_3(OH)$. Examination of the local environment of the constituent

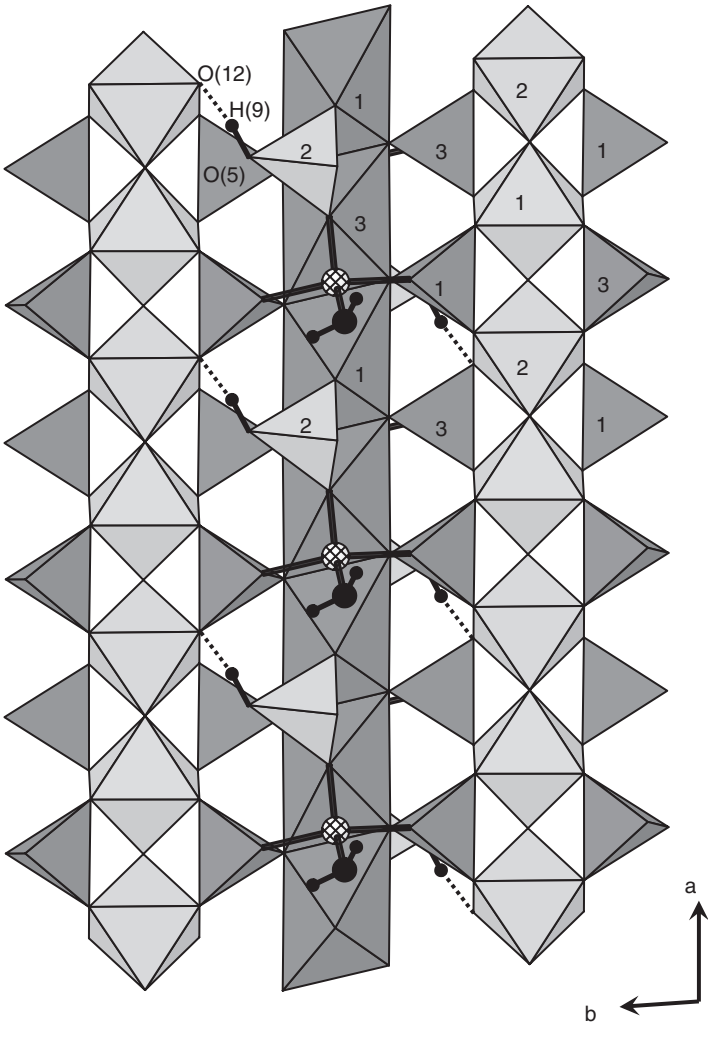

Figure 2. Linkage of $[(SbTi)(AsO_4)_4O_4]$ decorated corner-sharing chains by $[Cu_2(AsO_4OH)_2O_4]$ chains of edge-sharing Cu(1) and Cu(3) octahedra decorated with (AsO_4) tetrahedra to form a sheet parallel to (001). The cross-hatched circle denotes Cu(4), and the four shortest Cu-O bonds are shown by heavy lines. The oxygen atom of the (OH) group occurs at a corner of the As(2) tetrahedron, and the H(9) ... O(acceptor) bond is shown as a dotted line.

hydrogen atom, H(9), shows that it forms a hydrogen bond with O(5) (see tables 1, 2, figure 2).

Pairs of *trans* OW(1) and OW(2) (H_2O) groups bond to Cu(2). The Cu(2)–OW(1) distances are quite short (2.024 Å) whereas the Cu(2)–OW(2) distances are long (2.739 Å), resulting in [4+2]-coordination of Cu^{2+} at the Cu(2) site. The H(1) and H(2) atoms of the OW(1) group hydrogen bond to O(1) and O(4) of the $As(1)O_4$ tetrahedron (see table 2, figure 4a) and the H(3) and H(4) atoms of OW(2) hydrogen bond to O(2) of the $As(1)O_4$ tetrahedron and the OW(4) (H_2O) group. The H(3)...OW(4) and H(4)...O(2) hydrogen bonds are stronger than the hydrogen bonds involving OW(1) as the donor as O(2) is also bonded reasonably strongly to Cu^{2+} at Cu(4). The (H_2O)

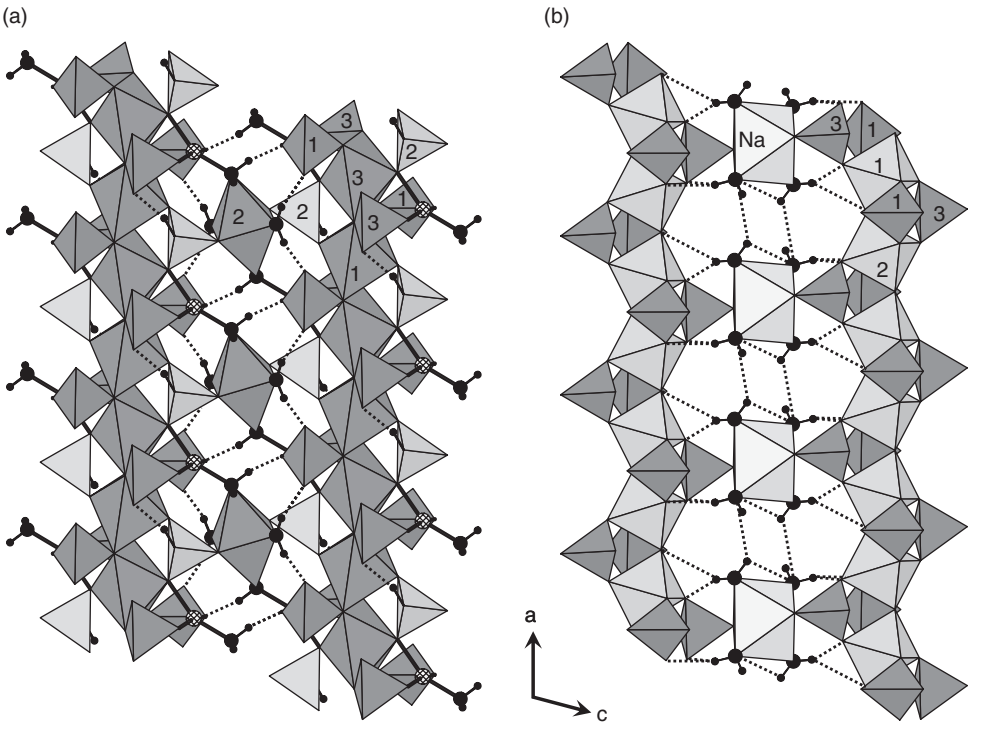

Figure 3. The connectivity of the structure in the ***c***-direction, showing linkage of the sheets portrayed in figure 2: (a) linkage at $z \approx 0$ where Cu(2) octahedra cross-link $[Cu_2(AsO_4OH)_2O_4]$ chains, together with extensive hydrogen bonding; (b) linkage at $z \approx 1/2$ where Na octahedra cross-link $[(SbTi)(AsO_4)_4O_4]$ chains, together with extensive hydrogen bonding. The atoms involved in hydrogen bonding are labeled, and hydrogen bonds are shown as dotted lines.

groups at OW(3) and OW(4) are both bonded to Na. The H(5) and H(6) atoms of OW(3) hydrogen bond to O(7) and O(1) + O(12), respectively (see tables 1, 2, figure 4b); note that H(6) forms a bifurcated hydrogen bond. The H(7) and H(8) atoms of OW(4) both form bifurcated hydrogen bonds, H(7) to O(10) and O(13), and H(8) to O(4) and OW(3). The resultant bond-valences incident at the anions are in accord with these hydrogen-bond arrangements.

3.4. *Relations with other structures*

The $[(SbTi)(AsO_4)_4O_2]$ chain shown in figure 1 may be generalized to $[M(TO_4)_2\Phi_4]_2$ (or more simply to $[M(TO_4)_2\Phi_4]$) where M is an unspecified octahedrally coordinated cation, T is an unspecified tetrahedrally coordinated cation, and Φ is an unspecified anion, usually O^{2-}, OH^-, F^-, Cl^- or (H_2O). A theoretical study of decorated corner-sharing chains of octahedra [11] derived the chain of figure 1 as one of the seven distinct arrangements possible with a repeat distance of two octahedra (~7 Å). This $[M(TO_4)_2\Phi_4]$ chain has since been found as a common building block in a wide variety of minerals.

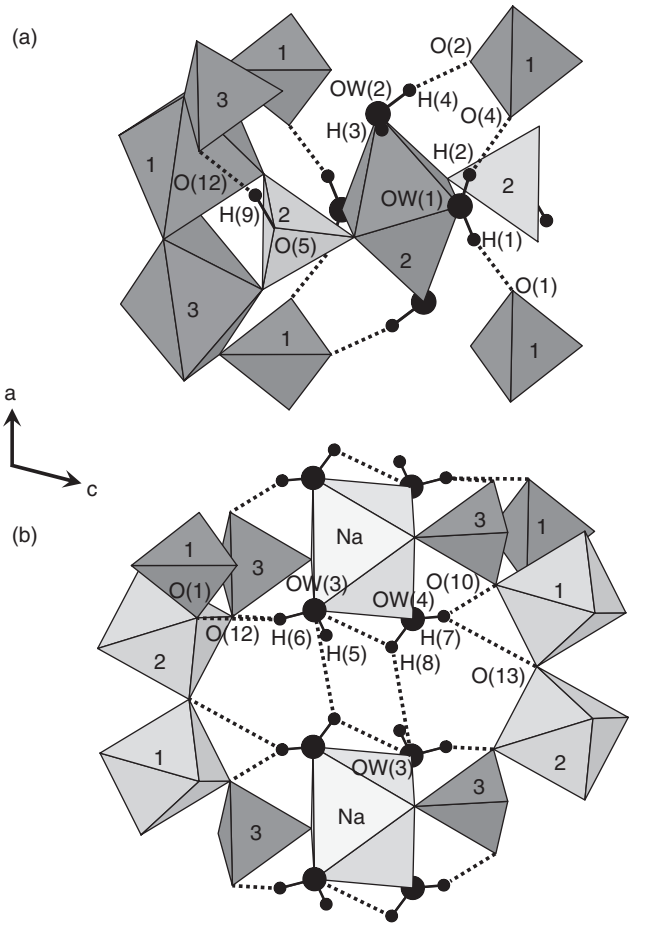

Figure 4. Hydrogen bonds in braithwaiteite: (a) OW(1) and OW(2); (b) OW(3) and OW(4). The oxygen atoms of the (H_2O) groups (labeled OW) are shown as large black circles, H atoms are shown as small black circles, O(donor)-H bonds are shows as heavy black lines, and H . . . O(acceptor) bonds are shown as dotted lines.

Anisodesmic crystal structures may be considered as binary objects in which strongly bonded *structural units* are linked into three-dimensional structures by weakly bonded *interstitial complexes* [12]. If we consider the $[M(TO_4)_2\Phi_4]$ chain as a building unit, there are three distinct types of structural units that may form: (1) simple $[M(TO_4)_2\Phi_4]$ chains; (2) sheets formed either by direct condensation of $[M(TO_4)_2\Phi_4]$ chains, or by linkage of $[M(TO_4)_2\Phi_4]$ chains by other strongly bonded atoms or groups of atoms; (3) frameworks formed either by direct condensation of $[M(TO_4)_2\Phi_4]$ chains, or by linkage of $[M(TO_4)_2\Phi_4]$ chains by other strongly bonded atoms or groups of atoms.

3.4.1. Chain structures. Perhaps the simplest chain structure is that of tancoite: $Na_2Li[Al(PO_4)(PO_3OH)(OH)]$ [13], in which the phosphate analogue of the chain shown in figure 1 is linked by Na, Li and a symmetrical hydrogen bond.

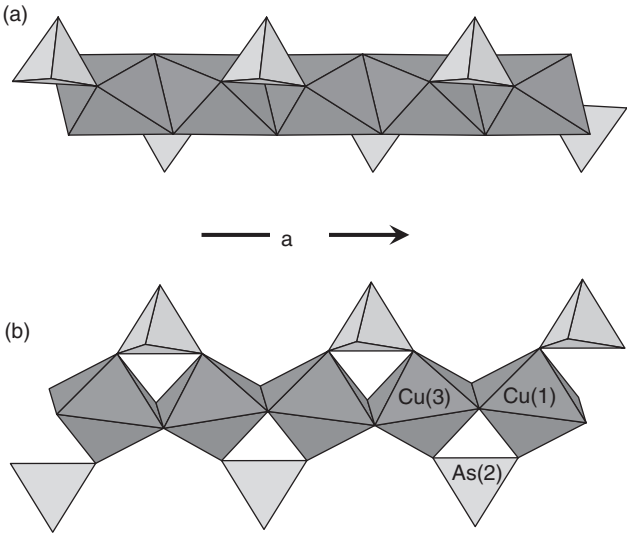

Figure 5. The $[Cu_2(AsO_4OH)_2O_4]$ chain in braithwaiteite (a) viewed perpendicular to the chain length and 20° from the ***b***-axis, and (b) viewed perpendicular to the chain length and 16° from the ***c***-axis.

Sideronatrite: $Na_2[Fe^{3+}(SO_4)_2(OH)](H_2O)_3$ [14], metasideronatrite: $Na_2[Fe^{3+}(SO_4)_2(OH)](H_2O)_{1.5}$ [15], and guildite: $Cu^{2+}[Fe^{3+}(SO_4)_2(OH)](H_2O)_4$ [16], are sulfate representatives. An extremely unusual structure is that of yftisite, $Y_4[Ti^{4+}(SiO_4)_2O](F,OH)_6$ [17], in which isolated $[Ti^{4+}(SiO_4)_2O]$ chains are linked by Y that also bond to monovalent anions not associated with the $[Ti^{4+}(SiO_4)_2O]$ chains.

3.4.2. Sheet structures. These are the most common structural types for minerals containing the $[M(TO_4)_2\Phi_4]$ chain, and some have several compositionally distinct mineral representatives. Minerals of the whiteite group, e.g. whiteite-(CaMnMg): $Mg_2(H_2O)_8$ $[CaMn^{2+}Al_2(PO_4)_4(OH)_2]$ [18], jahnsite-(CaMnFe^{2+}): $Fe^{2+}{}_2(H_2O)_8$ $[CaMn^{2+}Fe^{3+}{}_2(PO_4)_4(OH)_2]$ [19], consist of $[M(TO_4)_2\Phi_4]$ chains linked into sheets by Ca and Mn^{2+}. There is extensive geometrical isomerism in the linkage of the $[M(TO_4)_2\Phi_4]$ chains into sheets [19, 20] by $(MO_2(H_2O)_4)$ groups, giving rise to several groups of structurally distinct minerals, e.g. overite: $Mg(H_2O)_4[CaAl(PO_4)_2(OH)]$ [21], sinkankasite: Mn^{2+} $[Al(PO_3OH)_2(OH)](H_2O)_4$ [20].

In braithwaiteite, the $[(SbTi)(AsO_4)_4O_2]$ chains are linked by $[Cu_2(AsO_4OH)_2O_4]$ chains into a sheet (see figure 2). This chain is shown in figure 5; it may be generalized to $[M(TO_4)\Phi_2]$ which is a common element of several structures [22], including the minerals of the brackebuschite, $Pb^{2+}{}_2[Mn^{2+}(VO_4)_2(H_2O)]$ [23], fornacite, $Pb^{2+}{}_2[Cu^{2+}(AsO_4)(Cr^{6+}O_4)(OH)]$ [24], tsumcorite, $Pb^{2+}[Zn_2(AsO_4)_2(H_2O)]$ [25], and vauquelinite, $Pb^{2+}{}_2[Cu^{2+}(PO_4)(Cr^{6+}O_4)(OH)]$ [26], groups. It has a repeat distance of 5.67–6.18 Å, i.e. ~5.9 Å, in these minerals. The interesting feature of the $[M(TO_4)_2\Phi_4]$ and $[M(TO_4)\Phi_2]$ chains is that they have significantly different repeat distances along their length, and where they occur in the same structure, they perforce extend approximately orthogonal to each other. This is not the case in braithwaiteite. As is apparent in figure 2, the chains have the same repeat distance along their lengths, i.e. 7.0308 Å, the *a* dimension of the unit cell and the ideal repeat distance

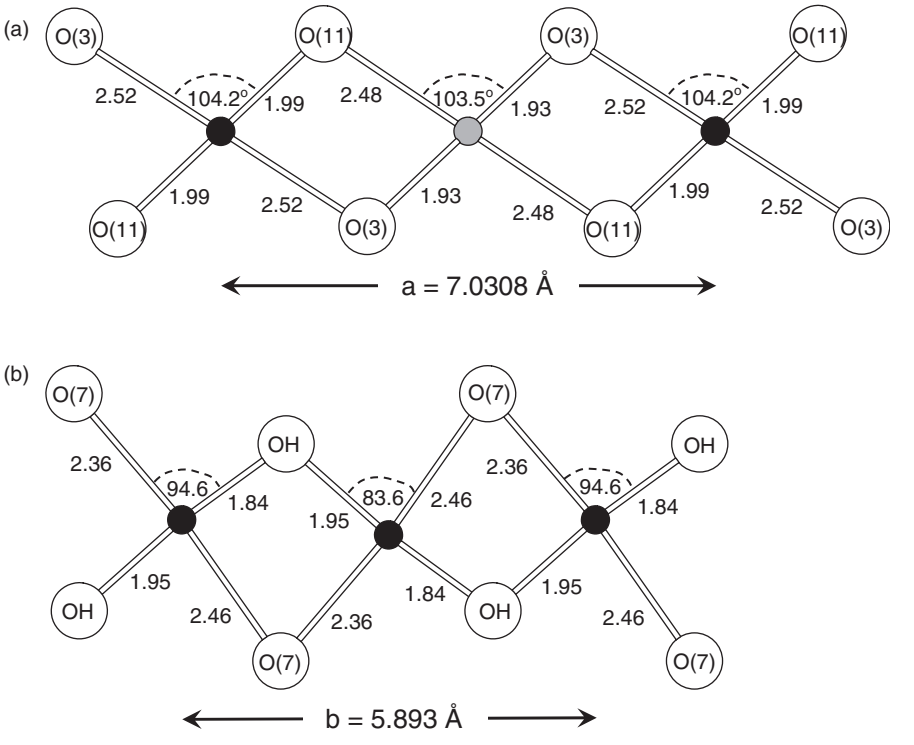

Figure 6. (a) a fragment of the $[Cu_2(AsO_4OH)_2O_4]$ chain in braithwaiteite, and (b) A fragment of the $[Cu^{2+}(AsO_4)\ (Cr^{6+}O_4)\ (OH)]$ chain in fornacite, showing selected bond lengths and angles.

of the $[M(TO_4)_2\Phi_4]$ chain. Although figure 5b best shows the structure of the $[Cu_2(AsO_4OH)_2O_4]$ chain, figure 5a shows how this chain extends its length. The mechanism is examined quantitatively in figure 6a. The Jahn-Teller distortions of the Cu(1) and Cu(3) octahedra are cooperatively oriented such that the octahedra extend in the same direction and the O-Cu-O angles open to ~104°, lengthening the chain sufficiently to extend it by one additional Å to match with the $[(SbTi)(AsO_4)_4O_2]$ chain. Note that fornacite contains a similar chain: $[Cu^{2+}(AsO_4)(Cr^{6+}O_4)(OH)]$, but the repeat length is only 5.893 Å (see figure 6b). Here, the Jahn-Teller distortion of the Cu octahedra orient differently and the associated O-Cu-O angles are much smaller than they are in braithwaiteite, i.e. mean values of 89.1° versus 103.9°.

A somewhat similar linkage occurs in goldquarryite, ideally $(Cu^{2+}_{0.5\square 0.5})Cd_2Al_3(PO_4)_4F_2(H_2O)_{10}(H_2O,F)_2$ [27], in which $[Al(PO_4)_2F]$ chains extend in the ***a***-direction and are cross-linked by chains of edge-sharing (CdO_6) octahedra to form strongly bonded sheets parallel to (001) (see figure 7).

3.4.3. Framework structures. There are fewer distinct types of framework structure containing the $[M(TO_4)_2\Phi_4]$ chain, but those that do show extensive solid-solution and numerous mineral representatives. In addition, they have received considerable attention as microporous materials [e.g. 28, 29]. Nenadkevichite, ideally

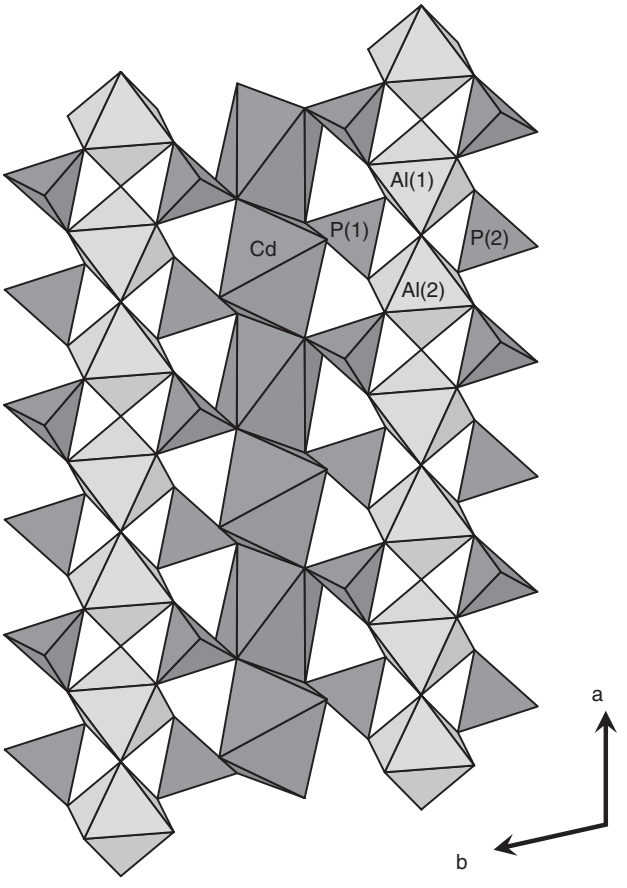

Figure 7. A sheet from the crystal structure of goldquarryite; $[Al(PO_4)_2F]$ chains extend parallel to ***a*** and are linked by chains of edge-sharing (CdO_6) octahedra. After Cooper and Hawthorne (2004).

$Na_2[Nb_2Si_4O_{12}\ O_2](H_2O)_4$ [30] and labuntsovite-Mg, ideally $Na_2K_2Mg[Ti^{4+}{}_4(Si_4O_{12})_2\ O_2(OH)_2](H_2O)_{5\text{-}6}$ [31] are titanium silicates containing $[Ti(SiO_4)_2(OH,O)]$ chains. These chains link by sharing vertices of tetrahedra (see figure 8) to form a framework in which $[Ti\Phi_5]$ chains are linked by $[Si_4O_{12}]$ rings to form a framework with one-dimensional channels extending in the ***c***-direction. There are several channel sites which can be occupied by alkali metals and small divalent cations such as Mg^{2+}, Fe^{2+} and Mn^{2+}, giving rise to many distinct mineral species [32].

3.5. *Relation between chemical composition and structure*

Inspection of the structures described in the above sections indicates some broad generalizations in terms of chemical composition and structure. In particular: (1) chain structures are generally sulfates (together with an acid phosphate, a pyrophosphate, and a yttrium silicate with monovalent anions not linked to the principal chain of the structure), (2) sheet structures are generally phosphates, arsenates and vanadates, and (3) frameworks are titanium silicates. We may interpret these regularities in terms of the

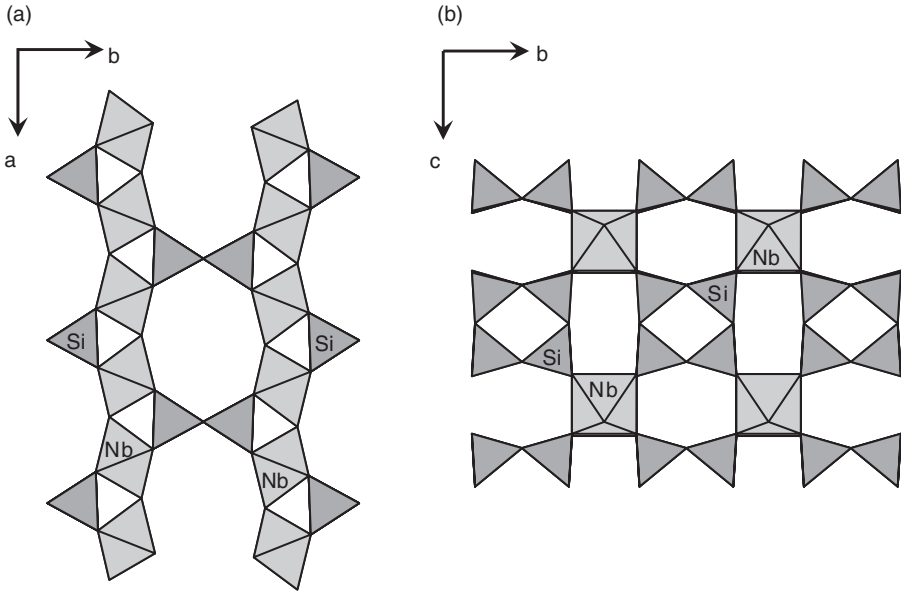

Figure 8. The crystal structure nenadkevichite: (a) the $[Ti(SiO_4)_4O_4]$ chains cross-linked by sharing vertices of the tetrahedra; (b) four $[Ti(SiO_4)_4O_4]$ chains link by sharing vertices of the tetrahedra to form a framework with channels parallel to ***a*** that contain the interstitial Na.

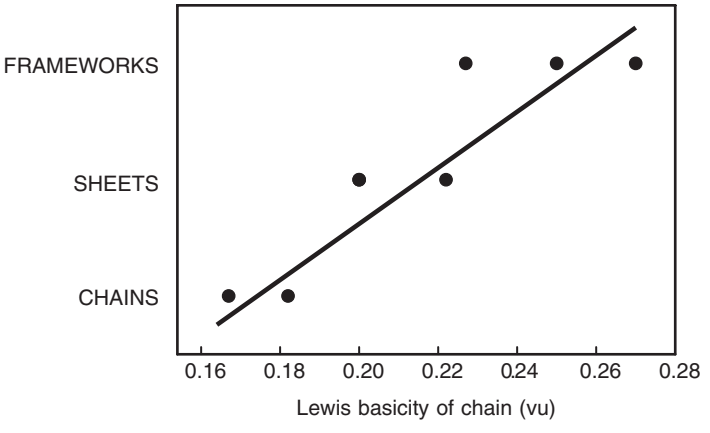

Figure 9. The mode of polymerization of the $[M(TO_4)_2\Phi_4]$ chain as a function of the Lewis basicity of the chain.

Lewis basicities of the structural units (the tightly bonded chain, sheet or framework parts of the structures) and the Lewis acidities of their interstitial complexes [33, 34, 35], the weakly bonded interstitial constituents of the structure. As shown in figure 9, the higher the Lewis basicity of the chain, the higher the degree of polymerization. This is a result of the fact that increasing polymerization decreases the Lewis basicity of the structural unit [22]. This is of significance because in order for a stable structure to form, the Lewis basicity of the structural unit must be approximately equal to the

Lewis acidity of the interstitial complex [12, 22, 33], and hence there is a cooperative interaction between the formation of the structural unit and the interstitial complex such that during crystallization, they both adjust their composition and structure to ensure that the valence-matching principle [12, 22, 33] is satisfied. Note that the $[Ti^{4+}(SiO_4)_2O]$ chain in yftisite, $Y_4[Ti^{4+}(SiO_4)_2O](F,OH)_6$, is not the $[Ti^{4+}(SiO_4)_2O]$ chain because there are relatively strong bonds between this chain and the Y that holds the chains together. Y has a Lewis-acid strength of 0.43 vu [33]. These interactions are too strong to be considered as interstitial, and hence yftisite is a framework structure; it plots on figure 9 accordingly.

Thus the degree of condensation of the $[M(TO_4)_2\Phi_4]$ chain in secondary oxysalt minerals is a function of the Lewis basicity of the chain, which in turn is a function of its bond topology and chemical composition.

Acknowledgements

This work was supported by a Canada Research Chair in Crystallography and Mineralogy, a Discovery grant and a Major Facilities Access grant from the Natural Sciences and Engineering Research Council of Canada and by Canada Foundation for Innovation grants to FCH.

References

[1] P. Keller, W.H. Paar, P.J. Dunn. *Tschermaks Min. Petr. Mitt.*, **28**, 157 (1981).
[2] F.C. Hawthorne. *Am. Mineral.*, **71**, 206 (1986).
[3] P.A. Williams. *Oxide Zone Geochemistry*, Ellis Horwood, Chichester, England (1990).
[4] D.E. Hibbs, P. Leveret, P.A. Williams. *Mineral. Mag.*, **67**, 47 (2003).
[5] R. Edwards, R.D. Gillard, P.A. Williams, A.M. Pollard. *Mineral. Mag.*, **56**, 53 (1992).
[6] J.L. Sharpe, P.A. Williams. *Austr. J. Mineral.*, **5**, 77 (1999).
[7] G.M. Sheldrick. *SHELX97. Program for the solution and refinement of crystal structures*, University of Göttingen, Germany (1997).
[8] I.D. Brown, D. Altermatt. *Acta Crystallogr.*, **B41**, 244 (1985).
[9] R. Eby, F.C. Hawthorne. *Acta Crystallogr.*, **B49**, 28 (1993).
[10] P.C. Burns, F.C. Hawthorne. *Can. Mineral.*, **34**, 1089 (1996).
[11] P.B. Moore. *Neues Jahrb. Min. Mh.*, **1970**, 163 (1970).
[12] F.C. Hawthorne. *Acta Crystallogr.*, **B50**, 481 (1994).
[13] F.C. Hawthorne. *Tschermaks Min. Petr. Mitt.*, **31**, 121 (1980).
[14] F. Scordari. *Tschermaks Min. Petr. Mitt.*, **28**, 315 (1981).
[15] F. Scordari, F. Stasi, G. Milella. *Neues Jahrb. Min. Monat.*, **1982**, 341 (1982).
[16] C. Wan, S. Ghose, G.R. Rossman. *Am. Mineral.*, **63**, 478 (1978).
[17] V.P. Balko, V.V. Bakakin. *Zhur. Strik. Khim.*, **16**, 837 (1975).
[18] P.B. Moore, J. Ito. *Mineral. Mag.*, **42**, 309 (1978).
[19] P.B. Moore, T. Araki. *Am. Mineral.*, **59**, 964 (1974).
[20] P.C. Burns, F.C. Hawthorne. *Am. Mineral.*, **80**, 620 (1995).
[21] P.B. Moore, T. Araki. *Am. Mineral.*, **62**, 692 (1977).
[22] F.C. Hawthorne. *Am. Mineral.*, **70**, 455 (1985).
[23] J. Foley, J.M. Hughes, D. Lange. *Can. Mineral.*, **35**, 1027 (1997).
[24] G. Cocco, L. Fanfani, P.F. Zanazzi. *Z. Kristallogr.*, **124**, 385 (1967).
[25] E. Tillmans, W. Gebert. *Acta Crystallogr.*, **B29**, 2789 (1973).
[26] L. Fanfani, P.F. Zanazzi. *Z. Kristallogr.*, **126**, 433 (1968).
[27] M.A. Cooper, F.C. Hawthorne. *Can. Mineral.*, **42**, 753 (2004).
[28] J. Rocha, P. Brandao, Z. Lin, A.P. Esculcas, A. Ferreira. *J. Phys. Chem.*, **100**, 14978 (1996).

[29] J. Rocha, P. Brandao, Z. Lin. *Chem. Comm.*, **1996**, 1359 (1996).
[30] G. Perrault, C. Boucher, J. Vicat, E. Cannillo, G. Rossi. *Acta Crystallogr.*, **B29**, 1432 (1973).
[31] N.I. Golovastikov. *Sov. Phys. Crystallogr.*, **18**, 596 (1974).
[32] N.V. Chukanov, I.V. Pekov, A.P. Khomyakov. *Eur. J. Mineral.*, **14**, 165 (2002).
[33] I.D. Brown. *The Chemical Bond in Inorganic Chemistry. IUCr Monographs in Crystallography* **12**, Oxford University Press, New York (2002).
[34] F.C. Hawthorne. In *The Stability of Minerals*, G.D. Price, N.L. Ross (Eds), p. 25, Chapman and Hall, London (1997).
[35] M. Schindler, F.C. Hawthorne. *Can. Mineral.*, **39**, 1225 (2001).